Topological Signature of Deterministic Chaos in Short Nonstationary Signals from an Optical Parametric Oscillator

Axelle Amon and Marc Lefranc

Laboratoire de Physique des Lasers, Atomes, Molécules, UMR CNRS 8523, Centre d'Études et de Recherches Lasers et Applications, Université des Sciences et Technologies de Lille, F-59655 Villeneuve d'Ascq, France

(Received 24 July 2003; published 5 March 2004)

Although deterministic chaos has been predicted to occur in the triply resonant optical parametric oscillator (TROPO) 15 years ago, experimental evidence of chaotic behavior in this system has been lacking so far, in marked contrast with most nonlinear systems, where chaos has been actively tracked and found. This situation is probably linked to the high sensitivity of the TROPO to perturbations, which adversely affects stationary operation at high power. We report the experimental observation in this system of a burst of irregular behavior of duration 80 μs. Although the system is highly nonstationary over this time interval, a topological analysis allows us to extract a clear-cut signature of deterministic chaos from a time series segment of only nine base cycles (3 μs). This result suggests that nonstationarity is not necessarily an obstacle to the characterization of chaos.

DOI: 10.1103/PhysRevLett.92.094101 PACS numbers: 05.45.–a, 42.65.Yj, 42.65.Sf

It has become common knowledge that many nonlinear systems obeying deterministic equations of motion can display seemingly erratic behavior. In the last decades, deterministic chaos has been the subject of intensive experimental investigation and has been observed in a large variety of experimental systems (see, e.g., [1]). However, characterizing chaos is significantly more demanding than characterizing periodic behavior, for which measuring simple quantities such as amplitude or frequency over a short time interval is sufficient. Indeed, most quantitative measures of chaos (e.g., fractal dimensions or Lyapunov exponents) rely on constructing an approximation of the natural measure on a strange attractor, which requires observing the system for at least a few hundreds of cycles at fixed control parameters [2,3].

Thus, it is extremely difficult to assess deterministic chaos in a system that experiences parameter drifts on a time scale comparable to the mean dynamical period, so that stationarity cannot be assumed. In particular, this is the case when studying a subsystem that cannot be considered as isolated from its environment, a situation that frequently occurs in biological systems. Yet, it is often desirable to understand the behavior of a small part of a complex system before unraveling its global dynamics. A natural question then is can we infer the existence of an underlying chaotic dynamics from a very short, nonstationary, time series? In this Letter, we present a case in which this question can be answered positively: by applying topological tools [4–6] to a burst of irregular behavior recorded in a triply resonant optical parametric oscillator (TROPO) subject to thermal effects, we extract a clear-cut signature of deterministic chaos from an extremely short time series segment of only nine base cycles.

Optical parametric oscillators are sources of coherent light based on parametric down-conversion of pump photons into pairs of subharmonic photons in a nonlinear optical crystal. This effect is enhanced by enclosing the crystal inside a cavity so as to build an oscillator. When the cavity is resonant for the three waves, the threshold for infrared generation can be as low as a few mW. As lasers, TROPOs are based on a nonlinear interaction and are naturally susceptible to instabilities and chaos. Accordingly, chaotic behavior was identified in a simple TROPO model 15 years ago [7]. Surprisingly, this theoretical prediction has so far not been confirmed experimentally.

Instabilities and chaos are expected to occur in the TROPO at high power, where optical nonlinearities are emphasized. However, high energy densities in the crystal induce other effects, in particular, thermal effects. It was recently shown that the TROPO can be subject to thermo-optical instabilities where the cavity length is no longer a fixed parameter but behaves as a slow variable coupled to the optical variables [8]. This gives rise to relaxation oscillations [8,9], as well as to a variety of bursting regimes [10] when these slow oscillations combine with fast oscillations resulting from the interaction of transverse modes [11]. The coexistence of two different time scales then makes it difficult to characterize the dynamics, especially in the case of irregular regimes.

The TROPO used in the experiment is as described in Refs. [8,9,11]. It features a 15-mm-long KTP (potassium titanyl phosphate) crystal cut for type-II phase matching, enclosed inside a 63-mm-long cavity delimited by two mirrors with a radius of curvature of 50 mm. Cavity length is not actively stabilized. The cavity is resonant at 532 nm, the wavelength of the frequency-doubled Nd:YVO_4 pump laser, and at 1064 nm, near which two infrared fields are generated. Parametric threshold is reached at pump powers of the order of 10 mW. At a pump power of 3.5 W (i.e., 350 times above threshold), we

have observed in the output signal intensity waveforms more complex than the periodic instabilities reported so far [8–12]. The time series that we analyze in this paper is shown in Fig. 1. Because the raw recording had limited vertical resolution, it has been processed through an acausal low pass filter with a cutoff frequency of 7 MHz. Acausal filtering of the time series has not been shown to introduce artifacts in subsequent phase-space reconstructions [13]. Between $t = 790$ μs and $t = 870$ μs, Fig. 1(a) displays a burst of irregular behavior inside a long interval of quasisinusoidal periodic behavior of frequency approximately 3 MHz. The rapid variation of the periodic waveform with time shows clearly that the system is highly nonstationary. The drift occurs on a time scale consistent with previous reports of thermal effects in this system [8,9].

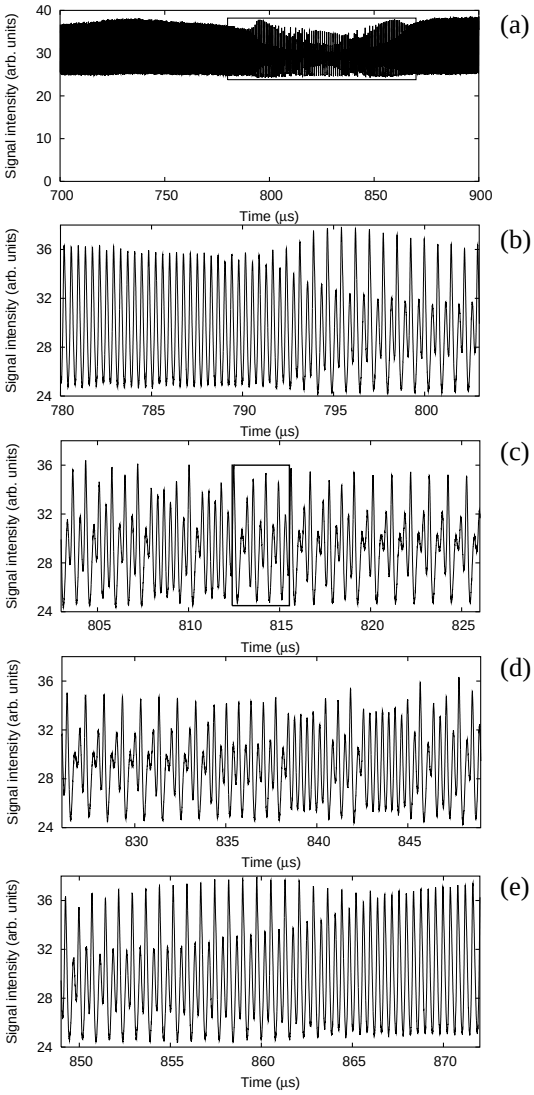

FIG. 1. (a) Signal intensity vs time; (b)–(e) consecutive excerpts from the irregular burst occurring for $t \in [780, 875]$. The segment between $t = 812.421$ and $t = 815.562$ contains a period-9 orbit used in the subsequent topological analysis.

The complex burst shown in detail in Figs. 1(b)–1(e) is highly suggestive of deterministic chaos. Between $t = 790$ μs and $t = 805$ μs, it begins by a progressive transition from the base period-1 orbit to a period-2 orbit. This is a signature of a period-doubling bifurcation, the first step of the most ubiquitous route to chaos. The reverse bifurcation can be seen in Fig. 1(e). Moreover, the time series displays a number of sequences of almost periodic behavior, a hallmark of low-dimensional chaos [4,5]. In particular, the segment between $t = 830$ μs and $t = 840$ μs contains three periodic bursts of periods 3, 2, and 1.

When chaotic behavior is suspected, a natural step is to try to reconstruct a strange attractor in a phase space using, e.g., the method of time delays [2–5]. In the present case, this procedure is questionable because the system is not stationary. Indeed, the superposition of trajectory segments corresponding to different values of control parameters is expected to yield a blurred plot. However, a phase-plane plot of the time series of Figs. 1(b)–1(e) is surprisingly similar to a Rössler-type chaotic attractor (Fig. 2). This indicates that trajectories of our system change their shape relatively slowly as a control parameter is varied.

Next, we choose a Poincaré section (Fig. 2) and construct a first return map for it. A convenient choice is the return map for the times of flight T_n between the nth and the $(n + 1)$th intersections with the section plane, which are relatively insensitive to noise. How T_n varies along the time series is shown in Fig. 3(a). This plot clearly displays the bifurcation diagram of a system that undergoes a period-doubling cascade, explores a chaotic zone followed by a period-3 periodic window, and then goes back. Note that the fraction of the diagram where complex behavior is observed is relatively small.

The plot (T_n, T_{n+1}) is shown in Fig. 3(b), where a folded structure similar to a one-dimensional map can easily be discerned. This suggests that the irregular

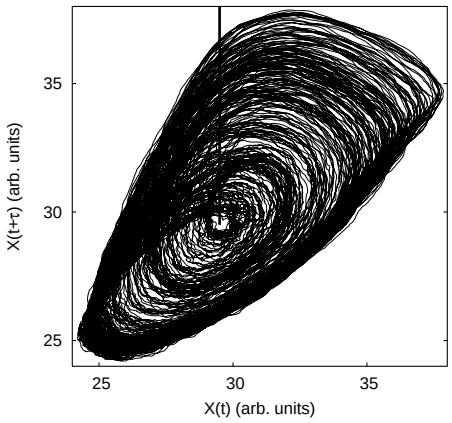

FIG. 2. Phase-plane portrait $[X(t), X(t + \tau)]$, with $X(t)$ the time series of Figs. 1(b)–1(e) and $\tau = 55$ ns. The vertical line indicates the section plane used in the subsequent analysis. Flow rotates clockwise around the hole in the middle.

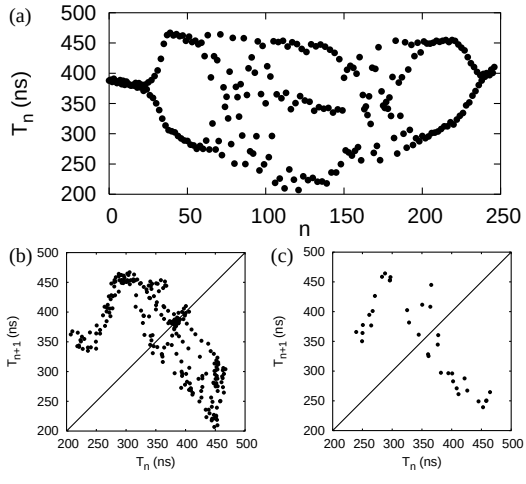

FIG. 3. (a) Poincaré section return times T_n vs intersection number n. Return maps (T_n, T_{n+1}) (b) for $n \in [1, 250]$; (c) for $n \in [70, 105]$.

dynamics observed in the experiment is deterministic. However, no quantitative information can be extracted from Fig. 3(b) which is blurred by variations in control parameters, as can be verified by plotting separately graphs corresponding to different parts of the time series. If we restrict ourselves to the first chaotic zone of Fig. 3 (i.e., for $n \in [70, 105]$, or $t \in [806.8, 819.0]$), the resulting plot is much closer to a one-dimensional map but there are now too few points to rigorously assess the presence of deterministic chaos, let alone to quantify it [Fig. 3(c)].

Indeed, most characterization methods require that the neighborhood of each point in phase space is sufficiently populated to capture the local structure of the attractor. Thus, they depend on the time series *nonlocally* in time: nearest neighbors in phase space are usually located far apart in the time series (*long-term recurrence*). This makes these methods fragile with respect to variations of control parameters along the time series. As we see below, a topological analysis circumvents this problem by extracting information from isolated time series segments, namely, those approaching a closed orbit (*short-term recurrence*): we shall not only extract a signature of an underlying chaotic dynamics in the fixed-parameter system but also obtain lower bounds on its topological entropy, a classical measure of chaos.

The time series of Fig. 1 displays many periodic events. As with the period-3 orbit, many of them correspond to stable periodic windows explored by the system as parameters are swept but some can also be found in zones of irregular behavior. They then likely correspond to a close encounter with one of the infinity of unstable periodic orbits embedded in a chaotic attractor.

The topological analysis of chaos [4,5] proceeds by characterizing the organization of periodic orbits, which are associated with closed curves in phase space. In dimension three, how these curves are intertwined can be studied using knot theory and branched manifolds (''templates''). This is because the knot invariants of periodic orbits provide topological signatures of the stretching and squeezing mechanisms organizing a strange attractor [4,5]. A major advantage of topological analysis is that each time series segment shadowing a periodic orbit, *stable or unstable*, can be analyzed independently of the others.

Although the time series of Figs. 1(b)–1(e) is very short, we have detected several closed orbits in it. The criterion was that the orbit should return to its initial condition in the (T_n, T_{n+1}) plane with 3% accuracy. These orbits are the period-1, period-2, period-4, and period-8 orbits of the period-doubling cascade, the period-3 orbit, as well as four orbits of periods 6, 7, 9, and 10.

We have found that the braids associated with these closed orbits can all be projected to a standard horseshoe template [4,5], as the structure of the return map suggests. More precisely, they have the same braid types as orbits 1, 01, 01^3, $01^3(01)^2$, 01^6, 011010111, $(011)^31$, 011, and 01^5 of the standard horseshoe template (ordered as in the time series). Linking numbers were not computed as this would require comparing different parts of the time series. This observation suggests that although orbits change their shape as control parameters vary along the time series, their topological organization is not modified. Such a robustness would be extremely unlikely if the irregular dynamics observed was not deterministic.

However, topological analysis can provide us with stronger evidence. Indeed, we have found that two of the closed orbits have a ''positive-entropy'' braid type. One is shown in Fig. 4. In a stationary system, how trajectories are stretched and folded around such an orbit forces the existence of an infinity of periodic orbits [6]. Thus, positive-entropy orbits exist only in systems that have experienced infinitely many bifurcations and are chaotic in some region of parameter space [4–6,14,15]: a ''pretzel knot'' (i.e., a common type of positive-entropy orbit

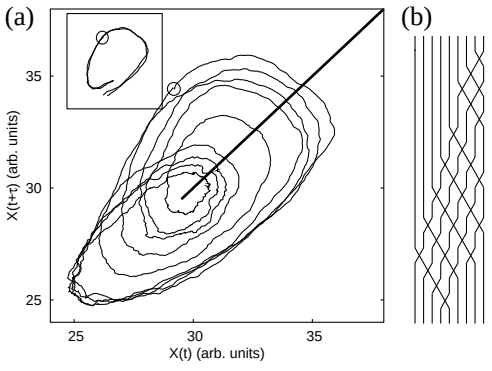

FIG. 4. (a) A period-9 closed orbit detected in the time series. The open circle indicates its starting and final points. The inset displays trajectory segments around these two points; (b) a presentation of this orbit as an open braid, using the diagonal as a Poincaré section.

having such a knot type) in a three-dimensional flow implies chaos just as a period-3 orbit in a one-dimensional map does. The presence of such an orbit in an experimental data set was first used as an indicator of chaos for the Belousov-Zhabotinskii reaction [16]. Pretzel knots have also been observed in laser experiments [17,18]. How many orbits are forced by a given braid type is quantified by its topological entropy, which is a lower bound on the topological entropy of systems containing it [6].

Using the TRAINS program by Hall [19], we have computed the topological entropy of the braid in Fig. 4(b) to be $h_T \sim 0.377\,057 > 0$. Similarly, the period-10 orbit has entropy $h_T \sim 0.473\,404 > 0$. If our system were stationary (as in Refs. [16–18]), the presence of such orbits would unambiguously imply chaos and provide a lower bound on topological entropy. However, the closed orbit in Fig. 4 is not a true periodic orbit, since control parameters have different values at its starting and final points.

Nevertheless, the following observation gives us confidence that the observed braid type is actually present in the unperturbed system. The inset of Fig. 4 shows two trajectory segments $\{X(t); t \in [t_0 - \tau_1, t_0 + \tau_2]\}$ and $\{X(t); t \in [t_0 + T - \tau_1, t_0 + T + \tau_2]\}$ centered around the starting point $X(t_0)$ and the ending point $X(t_0 + T)$ of the closed orbit, with $\tau_1 + \tau_2 = 350$ ns being approximately one orbital period. Although the two segments correspond to the extreme values of the control parameter along the closed orbit [Fig. 3(a) indicates that parameter variation is monotonic for $n \in [86, 93]$], we see that they are almost superimposed on each other. This indicates that the vector flow changes very little between $t = t_0$ and $t = t_0 + T$. The separation between the two segments can then be taken as an upper bound on the separation between the closed orbit observed and a periodic orbit of the unperturbed system. As this separation is significantly smaller than the separation between strands of the closed orbit in Fig. 4(a), the unperturbed system (i.e., the TROPO with fixed cavity length) must have a periodic orbit with the braid type shown in Fig. 4(b). We can then conclude that it exhibits deterministic chaos. Similarly, perturbations due to noise have no influence if their amplitude is small with respect to interstrand distance.

Our study shows that closed orbits with a positive-entropy braid type can be exploited when the influence of parameter variation is small over one orbit period, a modest requirement compared to other methods. However, we expect this approach to be also applicable to stronger nonstationarity. Generically, closed orbits of a system with a swept parameter connect continuously to periodic orbits of the unperturbed system as the sweeping rate goes to zero, as is easily shown using the implicit function theorem. If a positive-entropy closed orbit can be shown not to change its braid type along the homotopy path, then it provides a signature of chaos. Understanding when braid type is preserved is difficult, but a preliminary study of the logistic map with a swept parameter (where permutation of the periodic points is the counterpart of braid type) suggests that this approach is quite robust. Regarding applicability to higher-dimensional systems, where knots and braids fall apart, we are currently developing alternate methods for computing the topological entropy of a periodic orbit.

In conclusion, sophisticated topological methods have allowed us to obtain the first experimental signature of deterministic chaos in an optical parametric oscillator using only a very short segment of a nonstationary time series, which contained a positive-entropy orbit. Moreover, the fact that two such orbits were detected in less than 40 cycles indicates that these signatures of chaos are extremely robust with respect to variation in control parameters.

We thank R. Gilmore, T. Hall, S. Bielawski, D. Derozier, and J. Zemmouri for stimulating discussions. CERLA is supported by the Ministère chargé de la Recherche, Région Nord-Pas de Calais and FEDER.

[1] P. Cvitanović, *Universality in Chaos* (Adam Hilger, Bristol, 1989).
[2] E. Ott, *Chaos in Dynamical Systems* (Cambridge University Press, Cambridge, 1993).
[3] H. D. I. Abarbanel, *Analysis of Observed Chaotic Data* (Springer-Verlag, New York, 1996).
[4] R. Gilmore and M. Lefranc, *The Topology of Chaos: Alice in Stretch and Squeezeland* (Wiley, New York, 2002).
[5] R. Gilmore, Rev. Mod. Phys. **70**, 1455 (1998).
[6] P. Boyland, Topology Appl. **58**, 223 (1994).
[7] L. A. Lugiato, C. Oldano, C. Fabre, E. Giacobino, and R. J. Horowicz, Nuovo Cimento Soc. Ital. Fis. **10D**, 959 (1988).
[8] P. Suret, D. Derozier, M. Lefranc, J. Zemmouri, and S. Bielawski, Phys. Rev. A **61**, 021805(R) (2000).
[9] P. Suret, M. Lefranc, D. Derozier, J. Zemmouri, and S. Bielawski, Opt. Lett. **26**, 1415 (2001).
[10] A. Amon, M. Nizette, M. Lefranc, and T. Erneux, Phys. Rev. A **68**, 023801 (2003).
[11] P. Suret, M. Lefranc, D. Derozier, J. Zemmouri, and S. Bielawski, Opt. Commun. **200**, 369 (2001).
[12] C. Richy, K. I. Petsas, E. Giacobino, C. Fabre, and L. Lugiato, J. Opt. Soc. Am. B **12**, 456 (1995).
[13] F. Mitschke, Phys. Rev. A **41**, 1169 (1990).
[14] T. Hall, Nonlinearity **7**, 861 (1994).
[15] G. B. Mindlin, R. Lopez-Ruiz, H. G. Solari, and R. Gilmore, Phys. Rev. E **48**, 4297 (1993).
[16] G. B. Mindlin, H. G. Solari, M. A. Natiello, R. Gilmore, and X.-J. Hou, J. Nonlinear Sci. **1**, 147 (1991).
[17] F. Papoff, A. Fioretti, E. Arimondo, G. B. Mindlin, H. G. Solari, and R. Gilmore, Phys. Rev. Lett. **68**, 1128 (1992).
[18] M. Lefranc and P. Glorieux, Int. J. Bifurcation Chaos Appl. Sci. Eng. **3**, 643 (1993).
[19] T. Hall, TRAINS, software available from http://www.liv.ac.uk/maths/PURE/MIN_SET/CONTENT/members/T_Hall.html